DRUG DEVELOPMENT AND INDUSTRIAL PHARMACY, 16(17), 2465-2486 (1990)

THERMAL ANALYSIS OF POLYMERS

U.W. GEDDE, Department of Polymer Technology,
Royal Institute of Technology, S-100 44 Stockholm, Sweden

ABSTRACT

Thermal analysis embraces a group of analytical methods in which a physical property - e.g. enthalpy, mass, volume or birefringence - is measured as a function of temperature. This paper briefly presents differential scanning calorimetry (DSC), differential thermal analysis (DTA), thermogravimetry (TG), thermal mechanical analysis (TMA) and thermal optical analysis (TOA) as methods and describes in more detail their application on polymers. Examples are presented to demonstrate that the use of these methods and the interpretation of the results obtained requires special attention. The non-equilibrium nature of different polymers is illustrated by the melting and crystallization behaviour of flexible-chain polymers, the glass transition of amorphous polymers and phase transitions in liquid crystalline polymers. The information provided by thermal analysis about the morphology of crystalline polymers, the morphology of polymer blends and the chemical stability of polymers is also discussed.

INTRODUCTION

According to the definition originally proposed in 1969 (1) by the Nomenclature Committee of the International Confederation for Thermal Analysis (ICTA) and later reaffirmed in 1978 (2), thermal analysis includes a group of analytical methods by which a physical property of a substance is

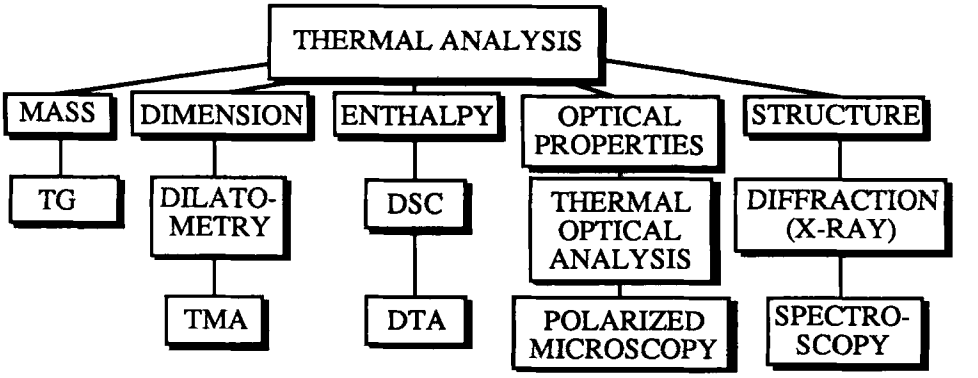

FIGURE 1. Thermo-analytical methods

measured as a function of temperature while the substance is subjected to a controlled temperature program. Thus, thermal analysis involves a physical measurement and not, strictly speaking, a chemical analysis. Figure 1 presents a summary of the different thermal analytical methods available. In this presentation, calorimetry, i.e. differential scanning calorimetry (DSC) and differential thermal analysis (DTA), thermogravimetry (TG), thermal mechanical analysis (TMA) and thermal optical analysis (TOA) are discussed. In the first section the methods are briefly described. The use of these methods on polymers requires special attention as is discussed in the final section of the paper. Examples from the melting and crystallization of flexible-chain polymers, the glass transition of amorphous polymers, phase transitions in liquid crystalline polymers and chemical reactions including the degradation of polymers are presented partly to illustrate the non-equilibrium effects which are typical of polymers.

Thermo-analytical methods are powerful tools in the hands of the polymer scientist. The number of phenomena which can be directly studied by thermal analysis (DSC (DTA), TG, TMA and TOA) is impressive. Typical of these methods is that only small amounts of sample (typically a few mg) is consumed by the analysis. Calorimetric methods record exo- and endothermic processes, e.g. melting, crystallization, liquid-crystalline phase transitions, and chemical reactions, e.g. polymerization, curing, depolymerization and degradation.

Second-order transitions, e.g. glass transitions, are readily revealed by the calorimetric methods. Thermodynamic quantities, e.g. the specific heat, are sensitively determined. TG is a valuable tool for the determination of the content of volatile species and fillers in polymeric materials and also for studies of polymer degradation. The majority of the aforementioned physical transitions can also be monitored by TMA (dilatometry). Additional information about the nature of the phase transitions in both crystalline and liquid crystalline polymers may be obtained by TOA.

THERMO-ANALYTICAL METHODS

The purpose of this paper is not to give the full details of the thermo-analytical methods. A very brief survey is however necessary in order to understand the later discussion of the phenomena in relation to polymers.

Calorimetry

Accurate temperature measuring techniques - thermocouple, resistance thermometer and optical pyrometer - were established in the late 1800's (3). These instruments were used by LeChatelier (4) in the late nineteenth century on chemical systems to study curves of change in heating-rate on clay. The first DTA method was conceived two years later by the English metallurgist Robert-Austen (5). The modern DTA instrumentation was introduced in 1951 by Stone (6). This apparatus permitted the flow of gas or vapour through the sample during the temperature scans. The undesirable feature of the classical DTA (Fig. 2b) in sensor-sample interaction was overcome by Boersma in 1955 (7). This type of instrument has since been referred to as "Boersma DTA" (Fig. 2c). The first differential scanning calorimeter was introduced in 1964 by Watson (8) of the Perkin-Elmer Co. A number of new developments in the instrumentation have been made during the last decades. The temperature scan is controlled and data are collected and analysed by computers in today's instruments. Simultaneous measurements of differential temperature (ΔT) and sample weight, i.e. combined DTA and TG as well as combined DTA and TOA are now commercially available (3). High-pressure DTA instruments have been in use for more than 20

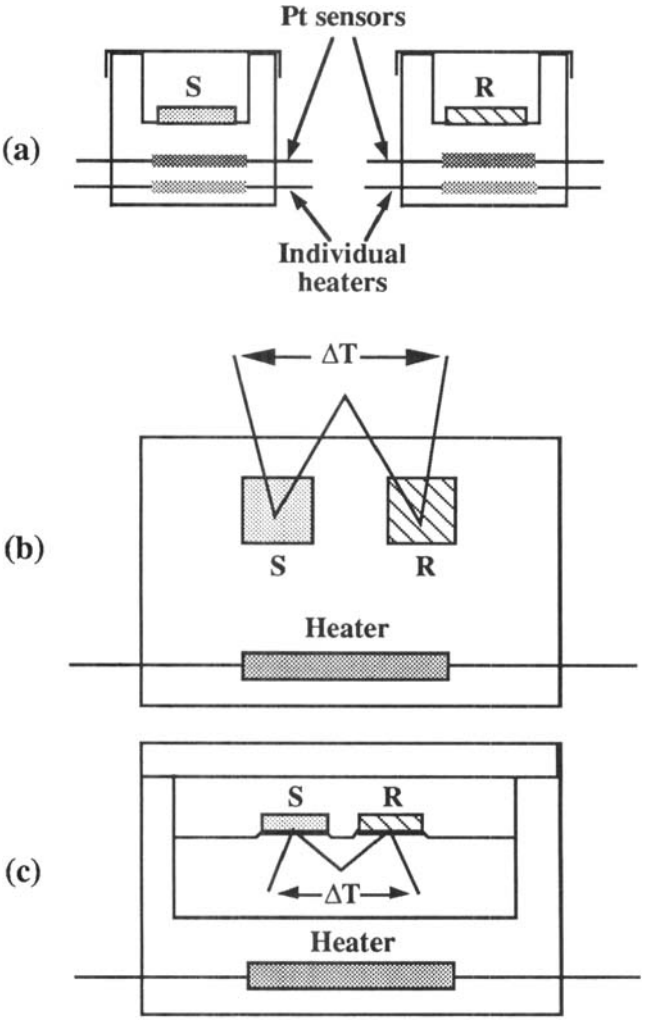

FIGURE 2. Schematic representation of (a) DSC, (b) "classical" DTA and (c) "Boersma" DTA. The notations for sample and reference are respectively "S" and "R".

years. Already in 1966, Cohen and coworkers (9) constructed a DTA cell which could be used at pressures up to 5 MPa. DSC instruments equipped with a UV cell are a more recent development (10). There are now more than 20 commercial DSC/DTA instruments available on the market.

A new class of highly sensitive (100 nW) isothermal or slowly scanning calorimeters to be used at temperatures lower than 120°C were developed by Wadsö and coworkers (11) starting in the late 1960's. The first instrument in the series was a batch reaction calorimeter (12). Similar systems had been made a few years earlier by Calvet and Prat (13) and Benzinger and Kitzinger (14). These thermopile heat conduction calorimeters consist of a calorimetric vessel surrounded by thermopiles, often consisting of Peltier elements through which the heat is conducted to or from the surrounding heat sink (11).

The calorimetric methods, DSC and DTA, are schematically presented in Fig. 2. DSC relies on the so-called "null-balance" principle (8). The temperature of the sample holder is kept the same as that of the reference holder by continuous and automatic adjustment of the heater power. The sample and reference holders are individually heated. A signal proportional to the difference between the heat power input to the sample and to the reference, dH/dt, is recorded. In the classical and Boersma DTA systems, sample and reference are heated by a single heat source. Temperatures are measured by sensors embedded in the sample and reference material (classical), or attached to the pans which contain the material (Boersma).

There are a few significant differences between DSC and DTA. The mass of the sample and reference holders in the DSC apparatus is very low and the maximum cooling rate is about one order of magnitude greater in the typical DSC apparatus than in DTA. The maximum measurement temperature for DSC is only about 725°C. The upper temperature limit for DTA instruments is significantly greater. This is however not a crucial question for organic polymers. One obstacle to calorimetric operation remains unsolved for the DTA; the factor converting observed peak area to energy is temperature dependent (3). This is particularly relevant for polymers which typically melt over a wide range in temperature. The melting curve is asymmetric requiring the use of a complex conversion factor. The calibration constant in DSC is independent of temperature and quantitative operation is inherently simpler than with DTA.

Thermogravimetry (TG)

The fundamental components of TG have existed for thousands of years. Mastabas or tombs in ancient Egypt (2500 B.C.) have wall carvings and paintings

displaying both the balance and the fire (15). The two components were however first coupled in the fourteenth century for studies of gold refining (16). Honda (17) pioneered in 1915 the modern TG analytical technique (thermobalance). The automatic thermobalance was introduced by Cahn and Schultz (18) in 1963. The number of commercial TG instrument models is presently more than 20.

TG is carried out in a so-called thermobalance which is an instrument permitting the continuous measurement of sample weight as a function of temperature/time. The following components are included in the typical TG instrument (3): (a) recording balance; (b) furnace; (c) furnace temperature controller; (d) computer. The furnaces can be run at temperatures up to 2400°C or more in a great variety of atmospheres, including corrosive gases (3). The sensitivities of the best modern recording balances are extremely good, in the range of μg (3). The strong development in the combined TG-Evolved Gas Analysis (IR, MS, GC, GC-IR and GC-MS) has recently been reviewed by Chiu (19).

Dilatometry/thermal mechanical analysis (TMA):

The classical way of measuring sample volume as a function of temperature is by a Bekkedahl dilatometer (20). More recent instrumentations, e.g. the thermal mechanical analysers (TMA) have been developed by several companies (3). These instruments not only measure volume and linear thermal expansion but also modulus as a function of temperature. When thermal expansion or penetration (modulus) is being measured the sample is placed on a platform of a quartz sample tube. The quartz tube is connected to the armature of a linear variable differential transformer (LVDT) and any change in the position of the armature is sensitively recorded. The upper temperature limit for the commercial instruments is about 725°C. Gillen (21) showed that the tensile compliance as obtained by TMA is comparable with the data measured by conventional techniques on considerably larger samples.

Thermal optical analysis (TOA)

TOA is normally carried out using a polarized microscope (crossed polarizers) equipped with a hot-stage by which the temperature of the sample can be

controlled. The microscopic image of the typically 10 μm thick sample can be directly viewed in binoculars or the transmitted light intensity can be recorded with a photodiode. Melting (crystallization) and mesomorphic phase transitions in liquid crystalline polymers can be directly studied by TOA. Apparatus for TOA of sheared polymer melts has been developed more recently, see e.g. (22).

THERMAL BEHAVIOUR OF POLYMERS

Crystalline polymers

The melting of polymer crystals exhibits many instructive features of non-equilibrium behaviour. It has been known since the 1950's that the crystals of flexible-chain polymers, e.g. polyethylene (PE), are lamellar-shaped with the chain-axis almost parallel to the normal of the lamella (23). The lamellar thickness (*L*) is of the order of 10 nm corresponding to approximately 100 main chain atoms, which is considerably less than the total length of the typical polymer chain (23). This fact led to the postulate that the macroconformation of the chains must be *folded* (23). The transverse dimensions (*B*) are two to three orders of magnitude greater than the lamellar thickness (23). The melting point (T_m) of thin lamellar crystals is controlled by the lamellar thickness (L) according to the Thomson-Gibbs equation, eq. (1):

$$T_m = T^\circ_m \left[1-\frac{2\sigma}{\Delta h^\circ \rho L}\right] \qquad \ldots.(1)$$

where T°_m is the melting point of the infinitely thick crystal, σ is the fold surface free energy, Δh° is the heat of fusion and ρ is the density of the crystalline component. Thus, factors, such as molecular mass, degree of chain branching and cooling rate may influence crystal thickness and hence the melting point.

The lamellar-shape (L/B≈ 0.01-0.001) of the polymer crystals is the reason for the rearrangement occurring at temperatures well below the melting point (Fig. 3). The equilibrium shape of the crystals can be calculated on the basis of the surface free energies of the fold surface (σ) and the lateral surface (σ_l):

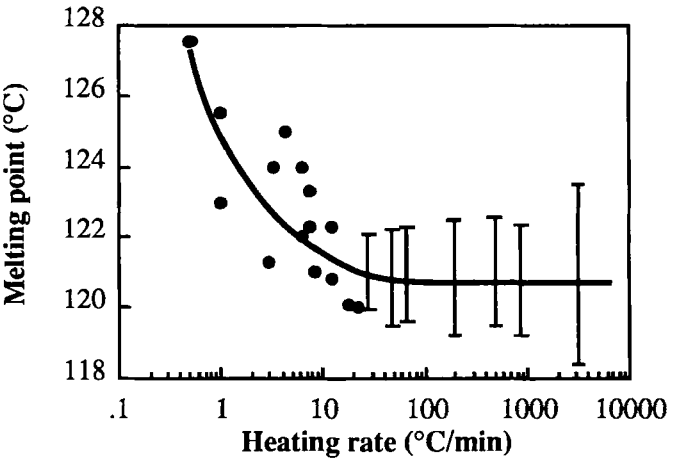

FIGURE 3. Melting point of solution crystals of LPE (0.05 % (m/m) in toluene at 81°C) as a function of heating rate. Drawn after data by Hellmuth and Wunderlich (26).

$$\frac{L}{B} = \frac{\sigma}{\sigma_l} \qquad \text{....(2)}$$

For linear polyethylene (LPE) the surface free energies are equal respectively to $\sigma = 93$ mJ(m)$^{-2}$ and $\sigma_l = 14$ mJ(m)$^{-2}$ (24) resulting in an equilibrium L/B value of 6.6 which is three orders of magnitude greater than the experimental value. The crystal thickening of polymer crystals expected to occur on the basis of these thermodynamic arguments has been verified by X-ray diffraction experiments (25). The recorded dependence of melting point on heating rate of single crystals of LPE presented in Fig. 3 is consonant with this view. At lower heating rates, the crystal thickening occurs to a much greater extent than at high heating rates which in turn leads to greater "final" crystal thickness and melting point after slow heating. The melting point value obtained at the higher heating rates is thus more consonant with that of the *original* crystals.

So-called extended-chain crystals are produced by high-pressure crystallization of linear polyethylene at elevated temperatures, typically at 0.5 MPa and 245°C (27). These very thick (μm) crystals display a distinctly

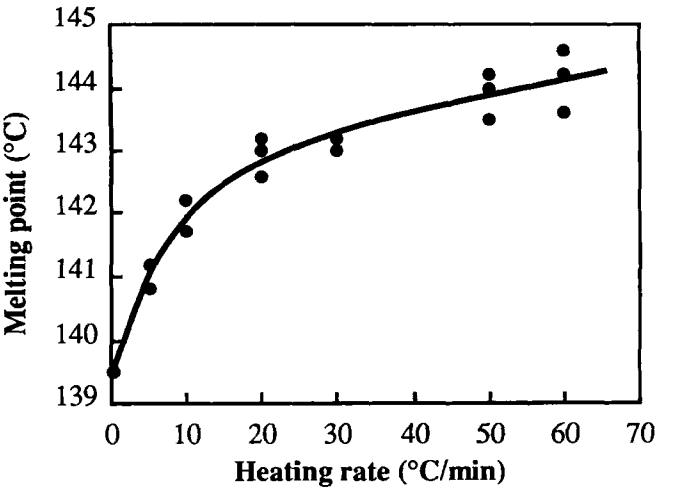

FIGURE 4. Melting point of extended-chain crystals of linear polyethylene (0.48 MPa; 227°C). Drawn after data by Hellmuth and Wunderlich (26).

different melting behaviour compared with that of the thin folded-chain single crystals grown from solution. The recorded increase in melting point with increasing heating rate shown in Fig. 4 is due to *superheating*. Crystals of intermediate thickness display approximately zero entropy production melting, i.e. melting point is almost independent of heating rate. Interestingly, as is shown in Fig. 5, linear polyethylene samples with a broad molecular mass distribution contain crystals of a great variety of crystal thicknesses displaying in a single sample reorganization, zero entropy production melting and superheating in order of increasing crystal thickness, i.e. melting point (28).

Polymers in general melt over a wide temperature range, typically covering more than 30°C. This may be due to a number of factors:

(a) The *multicomponent* nature (28-30): Polymers always exhibit a distribution in molecular mass and sometimes also in monomer sequence distribution (copolymers). The different molecular species crystallize at different temperatures which leads to a significant variation in crystal thickness and melting point. Polymer samples first crystallized under isothermal conditions and later rapidly cooled to lower temperatures frequently exhibit bimodal melting for

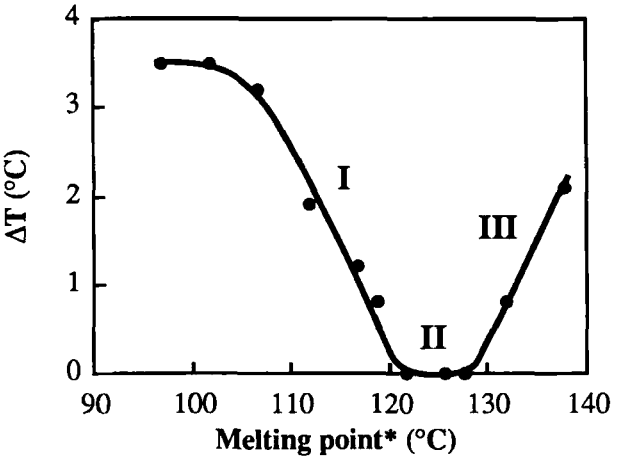

FIGURE 5. Difference (ΔT) in melting point as recorded at 10 K/min from that recorded at high heating rates (region I: crystal thickening) or zero heating rate (region III: superheating) plotted vs. melting point as recorded at 10 °C/min. . Region II refers to zero entropy production melting. Drawn after data by Gedde and Jansson (28) on linear polyethylene.

the aforementioned reasons. The high temperature peak is associated with the high molecular mass species which have crystallized at the isothermal conditions and the low temperature peak is due the low molecular mass component only able to crystallize during the subsequent cooling phase.

(b) *Reorganization* of crystals may occur on heating, either involving partial melting followed by crystallization forming thicker and more perfect crystals of essentially the same unit cell of the original crystals (31) or the transformation of one crystal structure to another (32-34). Samples which undergo these premelting transitional phenomena display bimodal or multimodal melting provided that the original crystals are of about the same lamellar thickness.

The content of crystalline component, the *crystallinity*, in the semi-crystalline polymers is a major factor affecting the material properties, e.g. modulus, permeability and density. The determination of the crystallinity of a sample can be made be several techniques, e.g. X-ray diffraction (35), density measurements (36) and DSC/DTA (37-39).

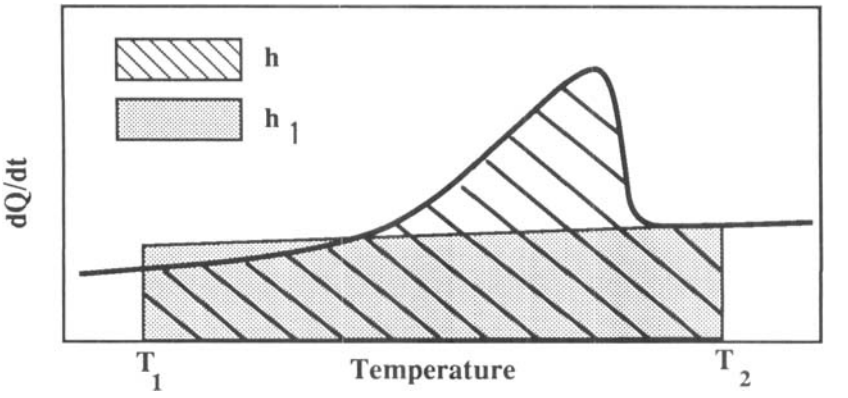

FIGURE 6. Schematic diagram of the DSC trace. Application of the total enthalpy method.

The mass crystallinity (w_c) obtained from the heat of fusion is based on the measurement of the area under the DSC melting peak. The choice of base line is crucial, most particularly so for polymers of low crystallinity, e.g. poly(ethylene terephthalate) (PETP). Another problem arises from the fact that the heat of fusion is temperature dependent. What temperature should be selected? Two rigorous methods have been proposed by Gray (37) and Richardson (38); (a) the total enthalpy method and (b) the peak area method. Excellent agreement is obtained for the crystallinity data on samples of linear, branched and chlorinated polyethylene and PETP obtained by DSC and the total enthalpy method with those obtained by X-ray diffraction (39). Referring to Fig. 6, the mass crystallinity at temperature T_1 is given by:

$$w_c(T_1) = \frac{h-h_1}{\Delta h°(T_1)} \qquad ....(3)$$

where $\Delta h(T_1)$ is the heat of fusion at temperature T_1 given by:

$$\Delta h°(T_1) = \Delta h°(T°_m) - \int_{T_1}^{T°_m} [c_{pa}-c_{pc}]dT \qquad ....(4)$$

where c_{pa} and c_{pc} are the specific heat of the amorphous and crystalline components. Specific heat data, i.e. c_{pa} and c_{pc} data on different polymers have been collected by Wunderlich and Baur (40).

Table 1. Derived values for the Avrami exponent (25)

Geometry	Athermal nucleation[a]	Sporadic nucleation[a]
Fibrillar	1 (0.5)	2(1)
Disc-shaped	2(1)	3(1.5)
Spherical	3(1.5)	4(2)

a) Constant growth rate; the values within brackets refer to diffusion controlled growth

Crystallinity determinations of polymers which degrade at low temperatures in the melting range constitute the most problematic case. Poly(vinyl chloride) belongs to this group and the base line definition is always a problem due to early thermal degradation and the low overall crystallinity which melts over a very broad temperature range (41).

The kinetics of crystallization, which is of interest for both academic and industrial reasons, are preferably studied under isothermal conditions by DSC, dilatometry or TOA. These methods reveal the overall crystallinity, volume (v_c) or mass (w_c) crystallinity as a function of time (t) and the general Avrami equation (eq. (5); n and K are constants and $v_{c\infty}$ is the maximum crystallinity attained) can be fitted to the data. An excellent review covering both fundamentals and practice of the Avrami equation is given by Wunderlich (25).

$$1-v_c/v_{c\infty} = \exp(-Kt^n) \qquad ...(5)$$

The Avrami exponent (n) depends on nucleation type, geometry of crystal growth and the kinetics of the crystal growth. Table 1 presents a few derived exponent values.

The kinetics at low degrees of conversion most frequently follow the Avrami equation but deviate from the linear trend in the $ln(-ln(1-v_c/v_{c\infty}))$ vs. lnt plot at higher degrees of conversion (25).

Most of the kinetic work has dealt with the temperature dependence of the growth rate in accordance with the kinetic theory of Lauritzen and Hoffman (24).

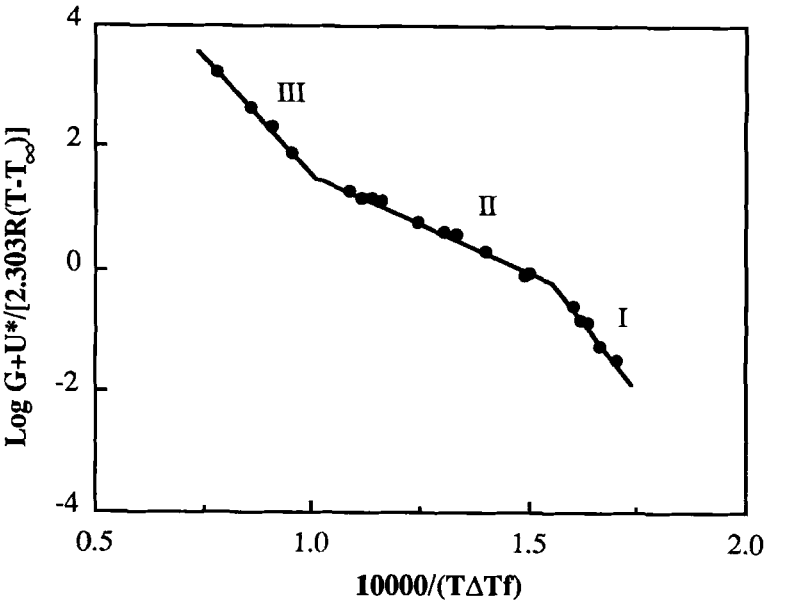

Figure 7. Crystallization kinetic data of linear polyethylene (42,43). The three rectilinear parts of the curve correspond to crystallization regimes I, II and III.

The experimental data, the linear growth rate (G) of the spherulites (axialites), is obtained by hot-stage polarized light microscopy at different constant temperatures and the data are adapted to eq. (6) in accordance with Fig. 7:

$$G = G_0 \exp\left[\frac{U^*}{R(T-T_\infty)}\right] \exp\left[\frac{-K_g}{T\Delta Tf}\right] \qquad ...(6)$$

where G_0 is a constant, U* is the activation energy for short-distance diffusion of the crystallizing segments, R is the gas constant, T is the crystallization temperature, T_∞ is a temperature which is related to the glass temperature, K_g is the "nucleation kinetic constant" which depends on the surface energies of the crystals formed the equilibrium melting point and the mechanisms of crystallization, ΔT is the degree of supercooling (= T°_m -T), and f is a correction factor near unity which corrects for changes in the heat of fusion with temperature.

A DSC analog to eq. (6) may be written as follows:

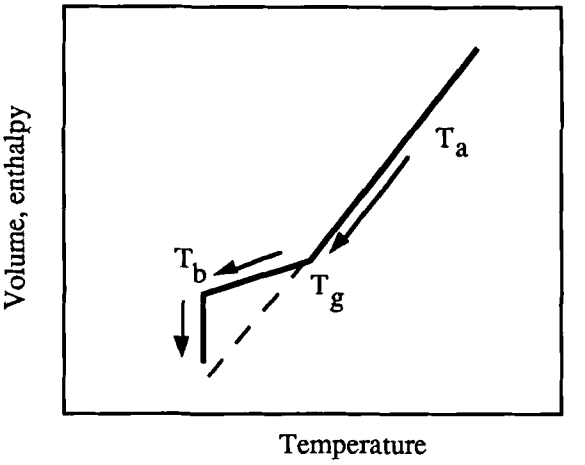

Figure 8. Schematic representation of the glass transition in amorphous polymers. The decrease in volume and enthalpy at T_b is referred to as physical aging.

$$t_{0.5}^{-1} = C \exp\left[-\frac{U^*}{R(T-T_\infty)}\right] \exp\left[\frac{-K_g}{T\Delta Tf}\right] \qquad ...(7)$$

where $t_{0.5}$ is the time corresponding to a 50% conversion and C is a constant. The former is obtained by DSC (DTA).

Amorphous polymers

The glass transition temperature is possibly the most prominent temperature for an amorphous polymer. The stiffness of a typical amorphous polymer changes by three orders of magnitude from a few GPa in the glassy state (low temperature side) to a few MPa in the rubbery state (high temperature side). The glass transition appears at first sight to be a second order phase transition, i.e. volume (V) and enthalpy (H) are continuous functions through the transition temperature (Fig. 8). However, if the amorphous polymer is cooled from temperature (T_a) a break on the rectilinear H,V=f(T) curve appears at the glass transition temperature (T_g). If the cooling is stopped at a temperature near T_g, at T_b in the Fig. 8, and the sample is kept at this temperature, H and V of the sample will decrease as a function of time. This so-called physical aging clearly shows that glassy amorphous polymers are not in equilibrium and that the

measured glass transition temperature is a "kinetic" temperature rather than being associated with a true thermodynamic transition. Physical aging thus leads to more densely packed material of higher stiffness and lower impact strength (44). The kinetics of physical aging can be followed by DSC/DTA and dilatometry. The fundamental aspects and practical implications of physical ageing have been the subject of many papers, e.g. by Struik (44) and Kovacs (45,46).

The non-equilibrium phenomena described above also cause a significant dependence on cooling rate of the recorded T_g. Atactic polystyrene, for example, shows a change in T_g from 365 K at a cooling rate of 1 K h^{-1} to 380 K at a cooling rate of 1 K s^{-1} (47). Even for a cooling rate of 1 K yr^{-1} the observed T_g does not decrease below 351 K (47). It is important to note that these data refer to the recorded T_g on cooling. On heating, glassy amorphous polymers exhibit superheating effects. If a slowly cooled amorphous polymer is rapidly heated, the T_g is shifted to significantly higher temperatures and an endothermic hysteresis peak is observed above the glass transition (47). In conclusion, the most reliable and precise way of measuring T_g is by cooling the melt at a specified low cooling rate and recording the step in the specific heat curve.

The morphology of amorphous polymer blends is indeed of great practical importance. The impact strength of stiff and brittle glassy polymers (e.g. atactic polystyrene) may be greatly improved by including a few percent of an *incompatible* elastomer like poly(butadiene). DSC(DTA) or TMA are, provided the polymers have different glass transition temperatures, valuable tools for seeking the answer to the crucial question of whether the polymers form a homogeneous solution or if they exist in different phases.

Fig. 9 shows the thermogram obtained from an incompatible mixture of styrene-acrylonitrile (SAN) and rubber-like polybutadiene. This blend is a high impact strength material referred to as acrylonitrile-butadiene-styrene (ABS) plastics. Two glass transitions are observed, the low temperature transition associated with the polybutadiene and the high temperature transition with the SAN copolymer (48).

Compatible blends are less commonly found. One of the most studied blends is that of polystyrene and poly(phenylene oxide) (PPO) (49). This blend is

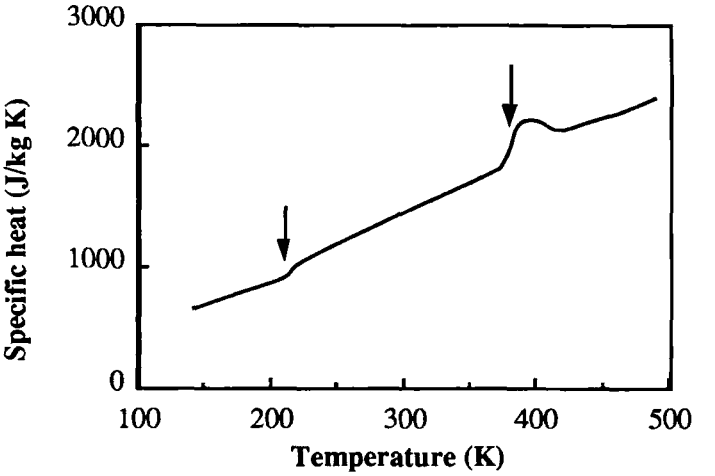

Figure 9. DSC thermogram of ABS showing two glass transitions. Drawn after data by Bair (51).

compatible in all proportions and the films of the blends are optically clear. Only one single glass transition intermediate in temperature between the T_g's of polystyrene and PPO has been reported (50-52). The compositional dependence of the T_g of a compatible binary blend follows in some cases, e.g. for blends of poly(vinyl chloride) and ethylene-vinyl acetate copolymers (53), the simple Fox equation (54):

$$\frac{1}{T_g} = \frac{w_1}{T_{g1}} + \frac{w_2}{T_{g2}} \qquad ...(8)$$

where w_i and T_{gi} is the weight fraction and glass transition temperature respectively of the pure polymers. There exist a great number of other equations relating T_g to the composition but the experimental data of many compatible binary blends are in disagreement with these equations (55).

Liquid crystalline polymers

Liquid crystalline (LC) polymers are a relatively new group of polymers which have aroused considerable interest during the last decade for two reasons. The so-called *main-chain* type, with the mesogenic stiff units implemented in the

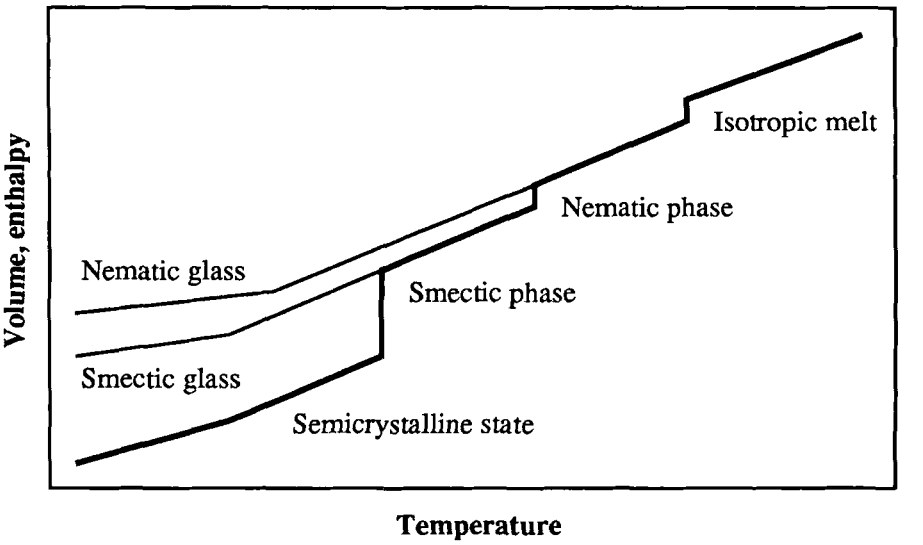

Figure 10. Phase transitions in thermotropic LC polymers

main chain exhibits a unique combination of good processing and mechanical properties and hence are now used as engineering plastics. The *side-chain* polymers with the mesogens in the side chains are mainly used in specialty functional polymers. LC polymers exhibit a number of thermal transitions as shown in Fig. 10.

Thermal analysis, DSC/DTA, TMA, TOA and hot stage microscopy are together with X-ray diffraction the methods which are available to reveal the thermal transition of the LC polymers. The combination of these methods is a prerequisite for structure/phase transition determination.

When it cools from very high temperatures, the isotropic melt is transformed into a liquid crystalline, so-called mesophase. A great number of different liquid crystalline structures have been reported (56, 57). Three major groups different in degree of order exist: nematic, cholesteric and smectic (56). The high temperature transition is readily revealed by DSC/DTA as an exothermic first order transition (see Fig. 10) and by TOA and hot stage polarized microscopy by the formation of birefringent structures. The phase assignment of the mesophase can be achieved

by polarized microscopy according to the scheme by Demus and Richter (56) or by X-ray diffraction (57). Ref. (57) is an excellent review dealing with the different methods now in use for characterization of thermotropic LC polymers.

At lower temperatures a number of liquid crystalline transitions may occur which again can be recorded by DSC/DTA as exothermic first order transitions (Fig. 10). Hot-stage microscopy and X-ray diffraction are used to determine the nature of these transitions. At even lower temperatures, solid crystals may be formed. The latter are revealed by DSC/DTA by the recording of an exothermic first order transition, by TMA by recording the increase in stiffness of the sample and by X-ray diffraction by recording sharp Bragg reflections. Some LC polymers, e.g. copolyesters are super-cooled to a glassy state without crystallizing (Fig. 10).

Polymer degradation

Thermoplastics are with very few exceptions very sensitive to degradation reactions occurring both during the melt processing and during use. Reactions with oxygen, thermal oxidation and photo-oxidation are for many polymers the dominating degradation reactions. Stabilisers, antioxidants, increase the stability of polymers and extend the life of many products to be great many years. The exposure of a plastic material to heat and oxygen leads to consumption of the antioxidant. It has therefore been of importance to develop efficient methods for the analysis of the antioxidant content. Thermal analysis, DSC/DTA and TG are among the most frequently used methods for this purpose.

The measurement of oxidative induction time (OIT) is made by first heating the polymer sample while keeping it in a nitrogen atmosphere at a high temperature, typically 200°C for polyethylene. After the establishment of constant temperature, the atmosphere is switched to oxygen and the time (OIT) to the start of an exothermic (oxidation) process is measured (Fig. 11). It has been shown that the OIT exhibits an Arrhenius temperature dependence (58,59) and that there is a linear relationship between OIT and the antioxidant content (60). It is important to note, that in order to use OIT data as an absolute method for the determination of the antioxidant content, the system must be calibrated. Similar

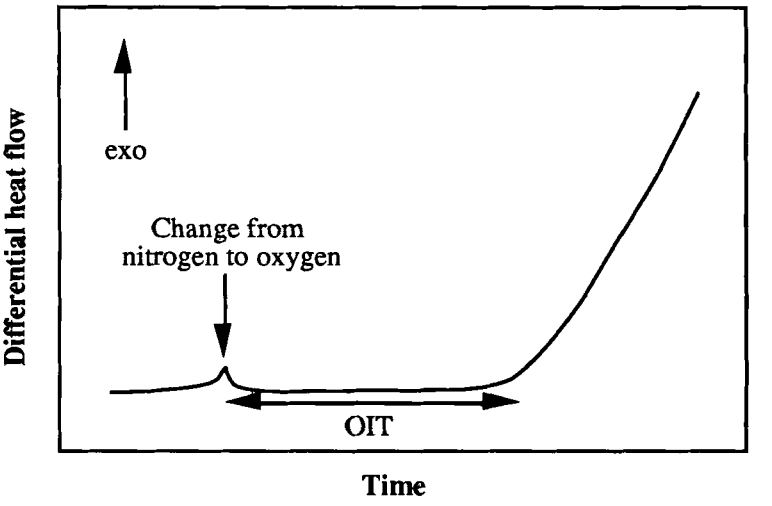

Figure 11. Typical thermogram from an OIT measurement

measurement can be made by TG (60). The first indication of oxidation is by a small increase in sample mass. At a later stage the sample mass decreases very strongly.

The antioxidant content can also be indirectly measured by recording the thermogram at a constant heating rate in an oxygen atmosphere, and a certain oxidation temperature (T_{ox}) may be established as the temperature of the exothermic deviation from the scanning base line (61).

ACKNOWLEDGMENTS

The financial support by the National Swedish Board for Technical Development (STU) and the Swedish Natural Science Research Council (NFR) during recent years involving thermal analysis of polymers is gratefully acknowledged. Dr. J. Suurkuusk, Thermometric AB, Järfälla, Sweden and Dr. I. Wadsö, Thermochemistry Laboratory, University of Lund, Sweden are gratefully thanked for valuable discussions concerning microcalorimeters.

REFERENCES

1. P.D. Gran, "Thermo-analytical Methods of Investigation", Academic Press, New York (1965).
2. W.W. Wendtlandt, "Thermal Methods of Analysis", 2nd Edition, Wiley, New York (1974).
3. W.W. Wendtlandt and P.K. Gallagher, "Instrumentation", in "Thermal Characterization of Polymeric Materials", Ed. E.A. Turi, Academic Press, New York (1981).
4. H. LeChatelier, Bull. Soc. Fr. Mineral Crystallogr., 10, 204 (1887).
5. W.C. Roberts-Austen, Metallographist, 2, 186 (1889).
6. R.L. Stone, Bull.- Ohio State Univ., Eng. Exp. Stn., 146, 1 (1951).
7. S.L. Boersma, J. Amer. Ceramic Soc., 38, 281 (1955).
8. E.S. Watson, M.J. O'Neill, J. Justin and N. Brenner, Anal. Chem., 36, 1233 (1964).
9. L.H. Cohen, W. Klement Jr. and G.C. Kennedy, J. Phys. Chem. Solids, 27, 179 (1966).
10. J. G. Kloosterboer, G.M.M. van de Hei, R.G. Gossink and G.C.M. Dortamt, Polymer Commun., 25, 354 (1984).
11. J. Suurkuusk and I. Wadsö, Chimica Scripta, 20, 155 (1982).
12. I. Wadsö, Acta Chem. Scand., 22, 927 (1968).
13. E. Calvet and H. Prat, in "Recent Progress in Microcalorimetry", Ed. H.A. Skinner, Pergamon Press, London (1963).
14. T.H. Benzinger and C. Kitzinger, in "Temperature - Its Measurement and Control in Science and Industry", Volume 3, Part 3, Ed. J.D. Hardy, Reinhold, New York (1963).
15. R. Vieweg, Prog. Vac. Microbalance Tech., 1, 1-24 (1972).
16. F. Szabadvary, in "History of Analytical Chemistry", p. 16, Pergamon Press, Oxford (1966).
17. K. Honda, Sci. Rep. Tohoku, 4, 95 (1915).
18. L. Cahn and H. Schulz, Anal. Chem., 35, 1729 (1963).
19. J. Chiu, "Thermogravimetry for Chemical Analysis of Polymers", in "Applied Polymer Analysis and Characterization: Recent Developments in Techniques, Instrumentation, Problem Solving", Ed. J. Mitchell Jr., Hanser Publishers, Munich (1987).

20. N. Bekkedahl, J. Research Natl. Bur. Standards, 43, 145 (1949).
21. K.T. Gillen, J. Appl. Polym. Sci., 22, 1291 (1978).
22. D.E Buerger, K. Engberg, J.-F. Jansson and U.W. Gedde, Polym. Bulletin, 22, 593 (1989).
23. B. Wunderlich, "Macromolecular Physics: Crystal structure, Morphology, Defects", Academic Press, New York (1973).
24. J.D. Hoffman, L.J. Frolen, G.S. Ross and J.I. Lauritzen Jr., J. Res. Natl. Bur. of Std., A6, 671 (1975).
25. E. Hellmuth and B. Wunderlich, J. Appl. Phys., 36, 3039 (1965).
26. D.C. Bassett and B. Turner, Phil. Mag., 29, 925 (1974).
27. U.W. Gedde and J.-F. Jansson, Polymer, 24, 1521 (1983).
28. U.W. Gedde, S. Eklund and J.-F. Jansson, Polymer, 24, 1532 (1983).
29. U.W. Gedde, J.-F. Jansson, G. Liljenström, S. Eklund, S.R. Holding, P.-L Wang and P.-E. Werner; Polym. Eng. Sci., 28, 1289 (1988).
30. B. H. Clampitt, J. Polym. Sci., 3, 671 (1965).
31. L. Mandelkern and A.L. Allou Jr., J. Polym. Sci., Polym. Phys. Edn., B4, 453 (1966).
32. J.L. Kardos, A.W. Christensen and E. Baer, J. Polym. Sci., Part A-2, 4, 447 (1966).
33. K.D. Pal, J. Polym. Sci., Part A-2, 6, 657 (1968).
34. P.J. Holdsworth and A. Turner-Jones, Polymer, 12, 195 (1971).
35. W. Ruland, Acta Cryst., 14,1180 (1961).
36. E. Hunter and W.G. Oakes, Trans. Faraday Soc., 41, 56 (1945).
37. A.P. Gray, Thermochimica Acta, 1, 563 (1970).
38. M.J. Richardson, Plastics and Rubber: Materials and Applications, 1, 162 (1976).
39. D.J. Blundell, D.R. Beckett and P.H. Willcocks, Polymer, 22, 704 (1981).
40. B. Wunderlich and H. Baur, Adv. Polymer Sci.,7, 151 (1970).
41. B. Terselius and J.-F. Jansson, Plast. Rubb. Proc. Appl., 5, 193 (1985).
42. J.M. Rego Lopez, M.T. Conde Braña, B. Terselius and U.W. Gedde, Polymer, 29, 1045 (1988).
43. J.D. Hoffman, Polymer, 24, 3 (1983).
44. L.C.E. Struik, "Physical Aging in Amorphous Polymers and Other Materials", Elsivier, Amsterdam, Oxfors and New York (1978).
45. A.J. Kovacs, Fortschr. Hochpolym. Forsch., 3, 394 (1964).

46. A.J. Kovacs, J.J. Aklonis, J.M. Hutchinson and A.R. Ramos, J. Polym. Sci., Polym. Phys. Ed., 17, 1097 (1979).
47. B. Wunderlich, D.M. Bodily and M.H. Kaplan, J. Appl. Phys., 35, 95 (1964).
48. H.E. Bair, Polym. Eng. Sci., 14, 202 (1974).
49. W.J. MacKnight, F.E. Karasz and J.R. Fried, in "Polymer Blends", D.R. Paul and S. Newman, Eds., Volume 1, p. 242, Academic Press, New York (1978).
50. H.E. Bair, Polym. Eng. Sci., 10, 247 (1970).
51. H.E. Bair, Anal. Calorim., 2, 51 (1970).
52. W.M. Prest and R.S. Porter, J. Polym. Sci., Polym. Phys. Ed., 10, 1639 (1972).
53. C.F. Hammer, Macromolecules, 4, 69 (1971).
54. T.G. Fox, Bull. Am. Phys. Soc., 1, 123 (1956).
55. S.W. Shalaby and H.E. Bair, in "Thermal Characterization of Polymers", E.A. Turi, Ed., p. 365, Academic Press, New York (1981).
56. D. Demus and L. Richter, "Textures of Liquid Crystals", VEB Deutscher Verlag für Grundstoffindustrie, Leipzig (1978).
57. C. Noël, in "Recent Advances in Liquid Crystalline Polymers", Ed. L. L. Chapoy, Elsivier Applied Science Publ., London and New York, p. 135 (1985).
58. J. B. Howard, Polym. Eng. Sci., 13, 429 (1973).
59. D.I. Marshall, E.J. George, J.M. Turnipseed and J.L. Glenn, Polym. Eng. Sci., 13, 415 (1973).
60. N.C. Billingham, D.C. Bott and A.S. Manke, in "Development in Polymer DEgradation", Volume 3, Ed. N. Grassie, P. 63, Applied Science Publ., London (1981).
61. U.W. Gedde and M. Ifwarson, Polym. Eng. Sci., 30, 202 (1990).